

Effects of nuclear correlations on the $^{16}\text{O}(e, e'pN)$ reactions to discrete final states

C. Barbieri*

*TRIUMF, 4004 Wesbrook Mall, Vancouver,
British Columbia, Canada V6T 2A3*

C. Giusti[†] and F. D. Pacati[‡]

*Dipartimento di Fisica Nucleare e Teorica dell'Università degli Studi di Pavia
and Istituto Nazionale di Fisica Nucleare, Sezione di Pavia, I-27100 Pavia, Italy*

W. H. Dickhoff[§]

*Department of Physics, Washington University,
St. Louis, Missouri 63130, USA*

(Dated: December 3, 2018)

Calculations of the $^{16}\text{O}(e, e'pN)$ cross sections to the ground state and first excited levels of the ^{14}C and ^{14}N nuclei are presented. The effects of nuclear fragmentation have been obtained in a self-consistent approach and are accounted for in the determination of the two-nucleon removal amplitudes. The Hilbert space is partitioned in order to compute the contribution of both long- and short-range effects in a separate way. Both the two-proton and the proton-neutron emission cross sections have been computed within the same models for the reaction mechanism and the contribution from nuclear structure, with the aim of better comparing the differences between the two physical processes. The $^{16}\text{O}(e, e'pp)$ reaction is found to be sensitive to short-range correlations, in agreement with previous results. The $^{16}\text{O}(e, e'pn)$ cross section to 1^+ final states is dominated by the Δ current and tensor correlations. For both reactions, the interplay between collective (long-range) effects and short-range and tensor correlations plays an important role. This suggests that the selectivity of $(e, e'pN)$ reactions to the final state can be used to probe correlations also beyond short-range effects.

PACS numbers: 21.10.Jx, 21.30.Fe, 21.60.-n, 25.30.Fj, 21.60.Jz.

I. INTRODUCTION

Among the various processes that characterize atomic nuclei, short-range correlations (SRC) play a very important role in the study of nuclear structure. It is now understood that the repulsive core of the nuclear interaction, at small distances, has a decisive influence on the spectral distribution of nucleons and on the binding properties of both finite and infinite nuclear systems [1–4]. Photo-induced two-nucleon knockout reactions like (γ, NN) and $(e, e'NN)$ appear to be a powerful tool to investigate two-body correlations in nuclei. Indeed, the probability that a real or virtual photon is absorbed by a pair should be a direct measure of the correlation between the two nucleons. The measurements of these cross sections have only become possible in recent years [5] by means of modern electron beam facilities. Studies with a ^{16}O target have been carried out at the AmPS-facility

at NIKHEF-Amsterdam [5–7] and the MAMI-facility in Mainz [8]. The comparison of the NIKHEF data with theoretical calculations [9, 10] for the $^{16}\text{O}(e, e'pp)$ reaction has been carried out in Refs. [6, 7]. In particular, it has been demonstrated that the transition to the ground state of ^{14}C is dominated by the presence of SRC whenever the two protons are emitted back-to-back with small total momenta. Therefore, the high experimental cross section observed for this transition at small missing momenta can be considered a clear signature of SRC [6, 7]. Further measurements have been carried out at the MAMI-facility in Mainz for the $^{16}\text{O}(e, e'pp)$ [8] reaction and proposed for the $^{16}\text{O}(e, e'pn)$ case [11]. The resolution achieved in these new experiments allows the separation of specific excited states in the residual nucleus.

A recent $(e, e'p)$ experiment [12, 13] performed at JLab also was aimed at the direct observations of high-momentum protons in the nucleus, another clear signature of SRC. These measurements are expected to produce new and detailed information on the one-body spectral distribution. However, due to the high missing energies and momenta required to observe this consequence of SRC, one is forced to work in a kinematic region where the effects of the final-state interaction tend to overwhelm the direct signal [12, 14]. The advantage of two-nucleon emission lies in the possibility of ejecting the correlated

*Electronic address: barbieri@triumf.ca; URL: <http://www.triumf.ca/people/barbieri>

[†]Electronic address: giusti@pv.infn.it

[‡]Electronic address: pacati@pv.infn.it

[§]Electronic address: wimd@wuphys.wustl.edu; URL: <http://www.physics.wustl.edu/~wimd>

pair as a whole, thus seeing the effects of SRC even at small missing energies and momenta but corresponding to large values of the relative momentum of the pair. On the other hand, several studies [10, 15, 16] suggest that details of the two-nucleon emission cross sections are sensitive not only to SRC. Indeed long-range correlations (LRC), at low energy, and the reaction mechanism are also important. Moreover, which of these effects is predominant depends on the particular choice of the kinematics and on the final state of the residual nucleus, in particular its angular momentum and parity. The latter quantities therefore act as a filter for the study of various reaction processes. Clearly, while this richness of details complicates the extraction of information related to SRC, it also identifies two-nucleon emission reactions as a unique tool to probe different aspects of two-body correlations in finite systems.

The model of the reaction mechanism employed in Ref. [10] was discussed in Ref. [17]. In this work the excitation process includes the contribution of the usual one-body terms as well as those two-body currents which involve the intermediate excitation of the Δ -isobar. In the present work the improved treatment of the nuclear currents, given in Refs. [18–20] will be employed. The treatment of the final-state interaction accounts for the distorting effect of their interaction with the remaining nucleons in terms of an optical potential. As in previous works, the mutual interaction between the two outgoing nucleons will be neglected here. This was argued in the past by noting that the pair of protons will leave the nucleus largely back to back making this type of final-state interaction less important. However, recent perturbative calculations on the $(e, e'pp)$ process [21–23] show that this effect can produce a significant increase of the experimental yield. Work is in progress to include these contributions completely [24]. This issue remains beyond the scope of the present investigation and will not be further discussed in the following.

An important element in the calculation of the cross section is the two-body overlap (or removal) amplitude, which contains the information on the correlations between the pair of nucleons inside the system. These amplitudes were computed in Ref. [25] for two protons by partitioning the full Hilbert space to obtain a model space large enough to account for the most relevant LRC. This is based on the assumption that the effects of SRC concern high relative momentum states (at high energy) and which are sufficiently decoupled from the collective motion at low energy as not to be influenced by it. The LRC were then obtained by solving the two-hole dressed random phase approximation (hh-DRPA) inside the model space, while the distortion due to SRC was included by adding appropriate defect functions, computed for the specifically excluded space. In doing so, the non-locality of the Pauli operator was neglected, resulting in a set of only few defect functions, essentially independent of the center-of-mass (c.m.) motion of the pair. The resulting two-nucleon spectral function was

then employed in the calculation of the $^{16}\text{O}(e, e'pp)$ cross section in Ref. [10]. A similar approach was followed in Ref. [15] for the $^{16}\text{O}(e, e'pn)$ case also by employing the same model [17–19] of the reaction mechanism. In this work the two-hole spectral function for a proton-neutron pair was obtained by employing a coupled-cluster approach. The S_2 approximation employed in Ref. [15] is quite similar to the evaluation of the short-range part of the two-body spectral function in terms of a Brueckner G matrix, as employed in Ref. [25], but does not account as well for the effects of LRC. However, a full set of defect functions, including their dependence on the c.m. of the pair, is obtained naturally in this approach. Given the differences between the above calculations, it is interesting to compare the emission of both a pp and a pn pair by evaluating them within the same description of the nuclear structure effects. Furthermore, the description of nuclear structure effects related to the description of the fragmentation of the single-particle strength has been improved by applying a Faddeev technique to the description of the internal propagators in the nucleon self-energy [26, 27]. This development provides an additional incentive to study the resulting consequences for the description of two-nucleon removal reactions. In the present work we pursue these aims by employing the hh-DRPA approach of Refs. [10, 25] while improving on the computation of the defect functions, in order to obtain a description of SRC comparable to the one of Ref. [15]. We then apply this model to study both the $^{16}\text{O}(e, e'pp)$ and $^{16}\text{O}(e, e'pn)$ reactions.

In Sec. II of this paper the essential steps in the calculation of the $(e, e'pN)$ cross sections are summarized. The calculation of the two-nucleon removal amplitudes, that describe the correlations, is discussed in Sec. III. There, the approach of separating the contributions of long-range (LRC) and short-range correlations (SRC) introduced in Ref. [28] is reviewed and the present calculation of defect functions is described in some detail. Sec. IIIA also summarizes the updated results for the nuclear structure calculation. The numerical results of $^{16}\text{O}(e, e'pp)$ and $^{16}\text{O}(e, e'pn)$ cross sections are presented and discussed in Sec. IV, while conclusions are drawn in Sec. V.

II. REACTION MECHANISM OF THE $(e, e'pN)$ CROSS SECTIONS

The coincidence cross section for the reaction induced by an electron with momentum \mathbf{p}_0 and energy E_0 , with $E_0 = |\mathbf{p}_0| = p_0$, where two nucleons, with momenta \mathbf{p}'_1 and \mathbf{p}'_2 and energies E'_1 and E'_2 , are ejected from a nucleus is given, in the one-photon exchange approximation and after integrating over E'_2 , by [29, 30]

$$\frac{d^8\sigma}{dE'_0 d\Omega dE'_1 d\Omega'_1 d\Omega'_2} = K \Omega_f f_{\text{rec}} |j_\mu J^\mu|^2. \quad (1)$$

In Eq. (1) E'_0 is the energy of the scattered electron with momentum \mathbf{p}'_0 , $K = e^4 p_0'^2 / 4\pi^2 Q^4$ where $Q^2 = \mathbf{q}^2 - \omega^2$, with $\omega = E_0 - E'_0$ and $\mathbf{q} = \mathbf{p}_0 - \mathbf{p}'_0$, is the four-momentum transfer. The quantity $\Omega_f = p'_1 E'_1 p'_2 E'_2$ is the phase-space factor and integration over E'_2 produces the recoil factor

$$f_{\text{rec}}^{-1} = 1 - \frac{E'_2}{E_B} \frac{\mathbf{p}'_2 \cdot \mathbf{p}_B}{|\mathbf{p}'_2|^2}, \quad (2)$$

where E_B and \mathbf{p}_B are the energy and momentum of the residual nucleus. The cross section is given by the square of the scalar product of the relativistic electron current j^μ and of the nuclear current J^μ , which is given by the Fourier transform of the transition matrix elements of the charge-current density operator between initial and final nuclear states

$$J^\mu(\mathbf{q}) = \int \langle \Psi_f | \hat{J}^\mu(\mathbf{r}) | \Psi_i \rangle e^{i\mathbf{q} \cdot \mathbf{r}} d\mathbf{r}. \quad (3)$$

If the residual nucleus is left in a discrete eigenstate of its Hamiltonian, i.e. for an exclusive process, and under the assumption of a direct knockout mechanism, the matrix elements of Eq. (3) can be written as [17, 30]

$$J^\mu(\mathbf{q}) = \int \Psi_f^*(\mathbf{r}_1 \sigma_1, \mathbf{r}_2 \sigma_2) J^\mu(\mathbf{r}, \mathbf{r}_1 \sigma_1, \mathbf{r}_2 \sigma_2) \times \Psi_i(\mathbf{r}_1 \sigma_1, \mathbf{r}_2 \sigma_2) e^{i\mathbf{q} \cdot \mathbf{r}} d\mathbf{r} d\mathbf{r}_1 d\mathbf{r}_2 d\sigma_1 d\sigma_2. \quad (4)$$

Equation (4) contains three main ingredients: the final-state wave function ψ_f , the nuclear current J^μ and the two-nucleon overlap integral ψ_i .

The nuclear current operator is the sum of a one-body and a two-body part. The one-body part contains the usual charge operator and the convective and spin currents. The two-body current is derived from the effective Lagrangian of Ref. [31], performing a non relativistic reduction of the lowest-order Feynman diagrams with one-pion exchange. We therefore have currents corresponding to the seagull and pion-in-flight diagrams and to the diagrams with intermediate Δ -isobar configurations [19], i.e.

$$\mathbf{J}^{(2)}(\mathbf{r}, \mathbf{r}_1 \sigma_1, \mathbf{r}_2 \sigma_2) = \mathbf{J}^{\text{sea}}(\mathbf{r}, \mathbf{r}_1 \sigma_1, \mathbf{r}_2 \sigma_2) + \mathbf{J}^\pi(\mathbf{r}, \mathbf{r}_1 \sigma_1, \mathbf{r}_2 \sigma_2) + \mathbf{J}^\Delta(\mathbf{r}, \mathbf{r}_1 \sigma_1, \mathbf{r}_2 \sigma_2). \quad (5)$$

Details of the nuclear current components and the values of the parameters used in the calculations are given in Refs. [18–20].

Equation (4) involves bound and scattering states, ψ_i and ψ_f , which should consistently be obtained from an energy-dependent non-Hermitian Feshbach-type Hamiltonian for the considered final state of the residual nucleus. They are eigenfunctions of this Hamiltonian at negative and positive energy eigenvalues, respectively [29, 30]. In practice, it is not possible to achieve this consistency and the treatment of initial and final state correlations proceeds separately with different approximations.

The final-state wave function ψ_f includes the interaction of each one of the two outgoing nucleons with the residual nucleus. The mutual interaction between the two outgoing nucleons has been studied in Ref. [21] in nuclear matter and, more recently, in two-nucleon knockout from ^{16}O in Refs. [22, 23] within a perturbative treatment. This contribution is neglected in the calculation of the present paper, which is aimed at investigating the effects of a consistent treatment of SRC and LRC in the initial state ψ_i . Therefore, the scattering state is here given by the product of two uncoupled single-particle distorted wave functions, eigenfunctions of a complex phenomenological optical potential [32] which contains a central, a Coulomb and a spin-orbit term. The two-nucleon overlap integral ψ_i contains the information on nuclear structure and correlations. These have been obtained using the same many-body approach for both pp and pn knock out, as described in the next section.

III. STRUCTURE AMPLITUDES

Following Ref. [10], the two-nucleon overlap integral ψ_i [see Eq. (4)] has been computed by solving the hh-DRPA equation for the two-particle Green's function. This approach allows to accurately take into account the effects of LRC that are important at the small missing energies considered in this work. However, the description of the high-momentum components due to SRC requires a large number of basis states, including configurations up to $100 \hbar\omega$ in an harmonic oscillator basis [33], which is too large for practical applications.

The guiding principle followed in the present calculation was presented earlier in Ref. [28] and attempts to treat LRC and SRC in a separate but consistent way. This is done by splitting the complete Hilbert space into a model space \mathcal{P} , large enough to contain the relevant long-range effects, and a complementary space $\mathcal{Q} = \mathbf{1} - \mathcal{P}$. The general formalism of the effective interactions considers a number of exact eigenstates of the system, $|\Psi_i\rangle$, that diagonalize the complete Hamiltonian $\hat{H} = \hat{T} + \hat{V}$ with eigenvalues E_i . One then seeks for an effective Hamiltonian \hat{H}_{eff} that is defined in the space \mathcal{P} and has the same exact eigenvalues (see for example Ref. [34]),

$$P \hat{H}_{eff} P |\Phi_i\rangle = E_i |\Phi_i\rangle, \quad (6)$$

where P is the projection operator onto the space \mathcal{P} and the eigenstates given by $|\Phi_i\rangle = P |\Psi_i\rangle$. The complete wave functions $|\Psi_i\rangle$, that belong to the full Hilbert space, can be obtained from the latter by means of

$$\begin{aligned} |\Psi_i\rangle &= (\mathbf{1} + \hat{\mathcal{X}}) |\Phi_i\rangle \\ &= |\Phi_i\rangle + |\mathcal{X}_i\rangle \end{aligned} \quad (7)$$

where the correlation operator $\hat{\mathcal{X}} = Q \hat{\mathcal{X}} P$ converts the component inside the model space into the corresponding

part that belongs to the space \mathcal{Q} . The latter, $|\mathcal{X}_i\rangle$, are usually referred to as “defect functions”.

In the present case, the nuclear correlations that lie in the space \mathcal{Q} are those due to SRC. For the case of two nucleons in free space the two-body correlations can be accounted for completely by solving the following equation for the transition matrix \hat{R} ,

$$\hat{R}(\omega) = \hat{V} + \hat{V} \frac{1}{\omega - \hat{T} + i\eta} \hat{R}(\omega), \quad (8)$$

where \hat{V} and \hat{T} are the NN potential and the kinetic energy, respectively, and ω is the energy of the correlated pair. A good approximation of the effective interaction, Eq. (6), that takes into account the effects of short-range distortion, is obtained by replacing the bare NN interaction \hat{V} with the G matrix, obtained by solving the Bethe-Goldstone equation

$$\hat{G}(\omega) = \hat{V} + \hat{V} \frac{Q}{\omega - Q\hat{T}Q + i\eta} \hat{G}(\omega). \quad (9)$$

Equation (9) accounts for the short-range effects in a way completely analogous to Eq. (8) except that the projection operator Q now allows the intermediate propagation of the two particles only within the space \mathcal{Q} (therefore excluding the correlations within the model space \mathcal{P}). The G matrix (9) plays the role of a transition matrix within the model space:

$$\hat{G}|\Phi\rangle = \hat{V}|\Psi\rangle, \quad (10)$$

where $|\Phi\rangle$ represents the two-body wave function within the space \mathcal{P} and $|\Psi\rangle$ is the fully correlated one that takes into account the distortion due to SRC. The latter regularizes the otherwise large matrix elements of \hat{V} that would be generated by its repulsive core at small interparticle distances. The correlated wave function is obtained in terms of the uncorrelated one $|\Phi\rangle$ as

$$|\Psi\rangle = |\Phi\rangle + \frac{Q}{\omega - Q\hat{T}Q + i\eta} \hat{G}(\omega)|\Phi\rangle, \quad (11)$$

which generalizes the Lippmann-Schwinger equation for two particles in the vacuum and gives an expression for the correlation operator $\hat{\mathcal{X}}$ of Eq. (7).

It should be noted that the distinction between long-range (inside the model space) and short-range correlations (outside the model space) is an artificial one. However, it is important to treat those contributions consistently and to avoid any kind of double counting. This is an important merit of the present approach [28]. The solution of the Bethe-Goldstone equation yields the residual interaction of the nucleons inside the model space as well as the defect functions needed to obtain the complete wave function, as in Eq. (7).

A. Two-nucleon overlap inside the space \mathcal{P}

The effects of LRC have been determined by performing a nuclear structure calculation within the same shell-

model space as employed in Ref. [27, 35], based on harmonic oscillator single-particle (sp) states with an oscillator parameter $b = 1.76$ fm (corresponding to $\hbar\omega = 13.4$ MeV). The space \mathcal{P} was chosen to contain all the first four major shells (from $0s$ to $1p0f$) plus the $0g_{9/2}$ orbital. The results of Refs. [35–39], suggest that this is large enough to properly account for the relevant low-energy collective states. The effective interaction (G matrix) was derived from the Bonn-C model of the NN potential \hat{V} [40]. Equation (9) was solved according to the method of Ref. [33] by first computing the real reaction matrix associated to \hat{R} , Eq. (8), in momentum space as a reference interaction. A correction term was then computed to account for the effects of the Pauli operator, which was treated in angle-averaged approximation.

The fragmentation of one-nucleon removal strength is described by the coupling of the fully dressed sp propagator to both two-particle (pp), two-hole (hh) and particle-hole (ph) excitations of the nuclear medium [27]. The simultaneous inclusion of all these collective modes into the nucleon self-energy Σ^* is computationally intensive and requires the solution of a set of Faddeev equations for the two-particle–one-hole and two-hole–one-particle motions [26]. This self-energy has been used to solve the Dyson equation for the one-body propagator

$$g_{\alpha\beta}(\omega) = g_{\alpha\beta}^0(\omega) + \sum_{\gamma\delta} g_{\alpha\gamma}^0(\omega) \Sigma_{\gamma\delta}^*(\omega) g_{\delta\beta}(\omega) \quad (12)$$

to obtain the one-nucleon removal spectroscopic factors for the low-energy final states in ^{15}N [25, 27]. In these works, the depletion of filled orbits by SRC is also incorporated in the shell-model space calculation by including the energy dependence of the G matrix interaction, which yields an energy-dependent Hartree-Fock term in the self-energy [25]. In Ref. [27], the collective pp (hh) and ph motion was studied at the level of the dressed RPA approximation by taking into account the fragmentation of the one-body spectral function. The propagator resulting from Eq. (12) was then substituted back into the calculation of the collective surface modes and in the Faddeev equations. This whole procedure was iterated until full self-consistency was obtained. The resulting description of the sp strength and corresponding two-hole states therefore represents an improvement of the description of LRC as compared to the work of Ref. [28]. Nevertheless, there are still features of the two-hole spectrum that cannot yet be described by the present method.

For the particular case of the two-hole motion, one solves the Bethe-Salpeter equation [41, 42] for the two-nucleon propagator G^{II} within the shell-model space. In the present hh-DRPA approach this reduces to

$$G_{\alpha\beta,\gamma\delta}^{II}(t_1, t_2, t_3, t_4) = i [g_{\alpha\gamma}(t_1 - t_3)g_{\beta\delta}(t_2 - t_4) - g_{\alpha\delta}(t_1 - t_4)g_{\beta\gamma}(t_2 - t_3)] \\ - \int_{-\infty}^{\infty} dt'_1 dt'_2 dt'_3 dt'_4 \sum_{\mu\nu,\kappa\lambda} [g_{\alpha\mu}(t_1 - t'_1)g_{\beta\nu}(t_2 - t'_2)] \langle \mu\nu | G(t'_1, t'_2, t'_3, t'_4) | \kappa\lambda \rangle G_{\kappa\lambda,\gamma\delta}^{II}(t'_3, t'_4, t_3, t_4), \quad (13)$$

where $\langle \mu\nu | G(t'_1, t'_2, t'_3, t'_4) | \kappa\lambda \rangle$ denote the elements of the G matrix interaction. From the Lehmann representation of the two-nucleon propagator G^{II} one obtains the reduced matrix elements of the two-nucleon removal tensor operators [41, 43, 44]

$$X_{abJ}^i = \langle \Psi_J^{i,A-2} | (c_{\beta}^i c_{\alpha}^i) | \Psi_0^A \rangle \quad (14)$$

where the latin subscripts denote the basis states without the magnetic quantum number, $a = \{n_{\alpha}, l_{\alpha}, j_{\alpha}\}$, and $\tilde{\alpha} = \{n_{\alpha}, l_{\alpha}, j_{\alpha}, -m_{\alpha}\}$ corresponds to the time reverse of α .

In Eq. (14), the quantities X_{abJ}^i represent the components of the two-nucleon overlap integral of Eq. (4) in the basis states of the model space. These can be expanded in terms of harmonic oscillator wave functions and transformed to a representation in terms of the relative and c.m. motion. For a discrete final state i of the (A-2)-nucleon system, with angular momentum quantum numbers JM , one obtains

$$\Phi_i(\mathbf{r}_1\boldsymbol{\sigma}_1, \mathbf{r}_2\boldsymbol{\sigma}_2) = \sum_{nlSjNL} c_{nlSjNL}^i R_{NL}(R) \\ \times \phi_{nl}(r) \left[\mathfrak{S}_{lS}^j(\Omega_r, \boldsymbol{\sigma}_1, \boldsymbol{\sigma}_2) Y_L(\Omega_R) \right]^{JM}, \quad (15)$$

where

$$\mathbf{r} = \mathbf{r}_1 - \mathbf{r}_2, \quad \mathbf{R} = \frac{\mathbf{r}_1 + \mathbf{r}_2}{2} \quad (16)$$

correspond to the relative and c.m. variables in coordinate space. Note that we follow the convention that denotes lower case for relative and upper case for c.m. coordinate quantum numbers. The brackets in Eq. (15) indicate angular momentum coupling of the angular and spin wave function \mathfrak{S} of relative motion with the spherical harmonic of the c.m. coordinate to the total angular momentum quantum numbers JM . The radial wave functions of the c.m. and relative motion are denoted by R_{NL} and ϕ_{nl} , respectively, and correspond to harmonic oscillators with parameters $b/\sqrt{2}$ and $\sqrt{2}b$ [45]. In Eq. (15), the nuclear structure information represented by the amplitudes X_{abJ}^i has been included in the coefficients

$$c_{nlSjNL}^i = \sum_{ab \in \mathcal{P}} \sum_{\lambda} \frac{(-)^{L+\lambda+j+S}}{\sqrt{2}} (2\lambda+1) \hat{j} \hat{S} \hat{j}_a \hat{j}_b \begin{Bmatrix} l_a & l_b & \lambda \\ s_a & s_b & S \\ j_a & j_b & J \end{Bmatrix} \\ \times \langle n l N L \lambda | n_a l_a n_b l_b \lambda \rangle \begin{Bmatrix} L & l & \lambda \\ S & J & j \end{Bmatrix} X_{abJ}^i, \quad (17)$$

$^{16}\text{O}(e, e'pp)^{14}\text{C}_{g.s.}$	n	N	ρ	Refs. [10, 28]	This work and Ref. [27]
$^1S_0; L=0$	0	1	2	-0.416	-0.410
	1	0	2	+0.415	+0.416
	0	0	0	+0.057	+0.039
	1	1	4	-0.069	-0.073
	0	2	4	+0.049	-0.006
	2	0	4	+0.050	+0.113
$^3P_1; L=1$	1	2	6	+0.016	+0.017
	2	1	6	-0.017	-0.017
	0	0	2	+0.507	+0.513
	0	1	4	+0.024	+0.076
$^1D_2; L=2$	1	0	4	-0.025	+0.019
	0	0	4	+0.016	+0.015

TABLE I: Two-proton removal amplitudes from ^{16}O to the ground state of ^{14}C , given in terms of a c.m. and relative motion expansion. The numbers in the left column are based on the Dressed RPA calculations described in Ref. [28], while those on the right account for the self-consistency in the nuclear self-energy obtained in Ref. [27]. The quantum number ρ corresponds to the total number of harmonic oscillator quanta of the pair: $\rho = 2n + l + 2N + L$ (lower case for relative and upper case for c.m. motion). For instance $\rho = 4$ indicates contributions from two holes in the sd shell.

where the notation $\hat{j} = \sqrt{2j+1}$ was used and the factor $1/\sqrt{2}$ has been inserted to be consistent with the normalization assumed in Eq. (4).

The most important amplitudes for the case of the transition to the ground state of ^{14}C are listed in Tab. I. These amplitudes are compared with the numbers in the left column, that refer to the calculation of Ref. [28]. The inclusion of the self-consistency effects in [27] (right column) does not substantially alter the results for these amplitudes, except for a slight enhancement of the collectivity of the 1S_0 contribution. Accordingly, the X_{abJ}^i principal components obtained for the pp case are essentially the same as those of Ref. [28]. In the calculation of Ref. [27], the spectroscopic factors for the removal of *one* nucleon from the $p_{1/2}$ and $p_{3/2}$ orbital of ^{16}O turned out to be reduced respectively by a factor of 0.72 and 0.76 as compared with the independent-particle shell model. This is still about 10% larger than the factor ~ 0.65 deduced from the experiments [46–48]. Given the competing effects of fragmentation and of the screening of the nuclear interaction, it is not clear a priori whether a re-

J^π	$(0p_{3/2})^{-2}$	$(0p_{3/2}, 0p_{1/2})^{-1}$	$(0p_{1/2})^{-2}$	$(0d_{5/2}, 0d_{3/2})^{-1}$
This work and Ref. [27]:				
1_1^+	0.033	-0.347	0.699	0.067
1_2^+	0.264	-0.680	-0.323	0.189
Ref. [15]:				
1_1^+	0.070	-0.455	0.607	
1_2^+	0.271	-0.544	-0.460	

TABLE II: Proton-neutron removal amplitudes X_{abJ}^i from ^{16}O to the first two states of ^{14}N . The numbers in the upper part of the table refer to the hh-DRPA results obtained in this work. For comparison, we give the analogous results obtained in the coupled cluster calculations of Ref. [15] (lower part). The normalization of the two-hole amplitudes is higher in the present work than what was assumed in Ref. [15].

duction of the spectroscopic factors will correspondingly reduce the two-nucleon emission cross sections. Therefore, as in previous work [10], we decided not to replace the calculated spectroscopic factors by the experimental ones in the present calculation.

The most relevant amplitudes X_{abJ}^i obtained for the emission of a pn pair are given in Tab. II, where they are compared with the analogous quantities from Ref. [15]. The results indicate that the mixing of the principal hole states is qualitatively similar in both calculations, although the hh-DRPA approach tends to favor the $(0p_{1/2})^{-2}$ and $(0p_{3/2}, 0p_{1/2})^{-1}$ components in the g.s. and first excited state of ^{14}N , respectively. The most important difference is that the present calculation predicts a sizable contribution for the emission of two nucleons from particle orbitals above the Fermi level. These components were not included in the approach of Ref. [15]. The sum of the squared amplitudes of Tab. II for the transition to the 1_1^+ and 1_2^+ states is 0.61 and 0.67, respectively, in the present approach and was 0.58 for both states in the coupled cluster calculation. The latter number was imposed in Ref. [15] by normalizing the amplitudes to the available DPRA results for the pp case [25]. The present calculation confirms this result for the pp channel but generates a higher normalization for the pn amplitudes. The above features introduced in the nuclear structure calculation generate important differences between the cross sections of Ref. [15] and the results discussed in Sec. IV B.

B. Calculation of the defect functions

In Eq. (17), the first sum runs over the sp states a and b that belong to the space \mathcal{P} . Thus the expansion in Eq. (15) is limited to configurations within this model space of two major shells above and two major shells below the Fermi level. The effects of correlations

on the overlap integral involving Ψ_i induced by the degrees of freedom outside the space \mathcal{P} can be included as in Eq. (7) [see also Eq. (11)]. The effects of SRC are due to close encounters of two nucleons, which mainly depend on the nuclear density and are not sensitive to the details of the long-range structure. Therefore we can assume that these processes are decoupled from each other. Since short-range effects involve high-momentum components, they pertain to the degrees of freedom in the space \mathcal{Q} which are described equivalently well by both the R and G matrices (since they differ mainly for their behavior inside the space \mathcal{P}). Therefore we substitute for \hat{G} in Eq. (11) the corresponding contribution generated by the standard Lippmann-Schwinger equation for \hat{R} [see Eq. (8)]. In the present work, we follow this prescription and compute the defect functions according to

$$|\mathcal{X}_i\rangle = Q \left\{ \frac{1}{\omega - \hat{T} + i\eta} \hat{R}(\omega) \right\} |\Phi_i\rangle, \quad (18)$$

where $|\phi_i\rangle$ is given by Eq. (15) and the operator Q ensures that all the correlations inside \mathcal{P} (generated by the term in curly brackets) are removed, thus avoiding any double counting. The operator R in Eq. (18) acts only on the radial part ϕ_{nl} of Eq. (15) leaving the contributions from R_{NL} untouched. The operator Q is computed exactly and in general can mix the quantum numbers of the relative and c.m. motion, however, without altering the form of the expansion (15). Thus the two-nucleon overlap amplitude Ψ_i appearing in Eq. (4) can be written as

$$\Psi_i(\mathbf{r}_1\boldsymbol{\sigma}_1, \mathbf{r}_2\boldsymbol{\sigma}_2) = \sum_{lSjNL} R_{NL}(R) \Psi_{lSjNL}^i(r) \times \left[\mathfrak{S}_{lS}^j(\Omega_r, \boldsymbol{\sigma}_1, \boldsymbol{\sigma}_2) Y_L(\Omega_R) \right]^{JM}, \quad (19)$$

where the complete radial components

$$\Psi_{lSjNL}^i(r) = \sum_n c_{nlSjNL}^i \phi_{nl}(r) + \mathcal{X}_{lSjNL}^i(r) \quad (20)$$

now include both the effects of LRC and SRC.

The defect functions employed in Ref. [10] were obtained by solving the Bethe-Goldstone only for specific partial waves in the relative motion and disregarding the dependence on the c.m. quantum numbers. This simplification also involves at least an angle-averaging approximation of the Pauli operator Q [33]. The approach followed here to compute exactly the operator Q in Eq. (18) allows to keep track of the dependence of \mathcal{X}_{lSjNL}^i on the c.m. degrees of freedom. Noting that the present interest concerns the high-momentum components due to SRC, it is natural to consider Eq. (18) as an improvement with respect to the approach of Ref. [10].

IV. RESULTS FOR PROTON-NUCLEON KNOCKOUT CROSS SECTIONS

In this section numerical results are presented for the cross sections of the reactions $^{16}\text{O}(e, e'pp)^{14}\text{C}$ and

$^{16}\text{O}(e, e'pn)^{14}\text{N}$ to the lowest-lying discrete states in the residual nucleus that are expected to be strongly populated by direct knockout of two nucleons. The main aim of this study is to investigate the role of correlations, that are consistently included in the two-nucleon overlap amplitudes for the proton-proton and the proton-neutron emission processes. Of particular interest is also the comparison with the $(e, e'pp)$ results of Ref. [10], as the present approach represents an improvement, and with the $(e, e'pn)$ results of Ref. [15], where a different description was used to calculate the proton-nucleon overlap amplitudes.

A. The $^{16}\text{O}(e, e'pp)^{14}\text{C}$ reaction

Calculations have been performed for three low-lying positive parity states of ^{14}C : the 0^+ ground state, the 1^+ state at 11.3 MeV, and the 2^+ state at 7.67 MeV, which corresponds to the two 2^+ states at 7.01 and 8.32 in the experimental spectrum [49]. These states are of particular interest since they can be separated in high-resolution experiments [5–8].

As an example, we have considered the so-called super-parallel kinematics [30], where the knocked-out nucleons are detected parallel and antiparallel to the transferred momentum \mathbf{q} . In this kinematics, for a fixed value of the energy and momentum transfer it is possible to explore, for different values of the kinetic energies of the outgoing nucleons, all possible values of the recoil momentum.

The super-parallel kinematics is favored by the fact that only two structure functions, the longitudinal and transverse ones, contribute to the cross section. These can in principle be separated by a Rosenbluth plot in a way analogous to the inclusive electron scattering [30]. This kinematical setting is also favorable from the experimental point of view. It has been realized in a recent $^{16}\text{O}(e, e'pp)^{14}\text{C}$ experiment at MAMI [8] and has been proposed for the first experimental study of the $^{16}\text{O}(e, e'pn)^{14}\text{N}$ reaction [11]. The choice of the same kinematics for proton-proton and proton-neutron emission is of particular interest for the comparison of cross sections and reaction mechanisms and for the investigation of correlations and of their contributions in the two processes.

The calculated differential cross sections of the reaction $^{16}\text{O}(e, e'pp)$ to the three final states in super-parallel kinematics are displayed in Fig. 1. The separate contributions of the one-body and the two-body Δ current are also shown in the figure. Note that the seagull and pion-in-flight meson-exchange currents do not contribute in proton-proton emission, at least in the nonrelativistic limit considered here.

It was widely discussed in previous studies [5, 10] how resolution of discrete final states may provide a tool to discriminate between contributions from one-body currents, due to SRC, and two-body currents. The results in Fig. 1 confirm the selectivity of the $^{16}\text{O}(e, e'pp)^{14}\text{C}$ re-

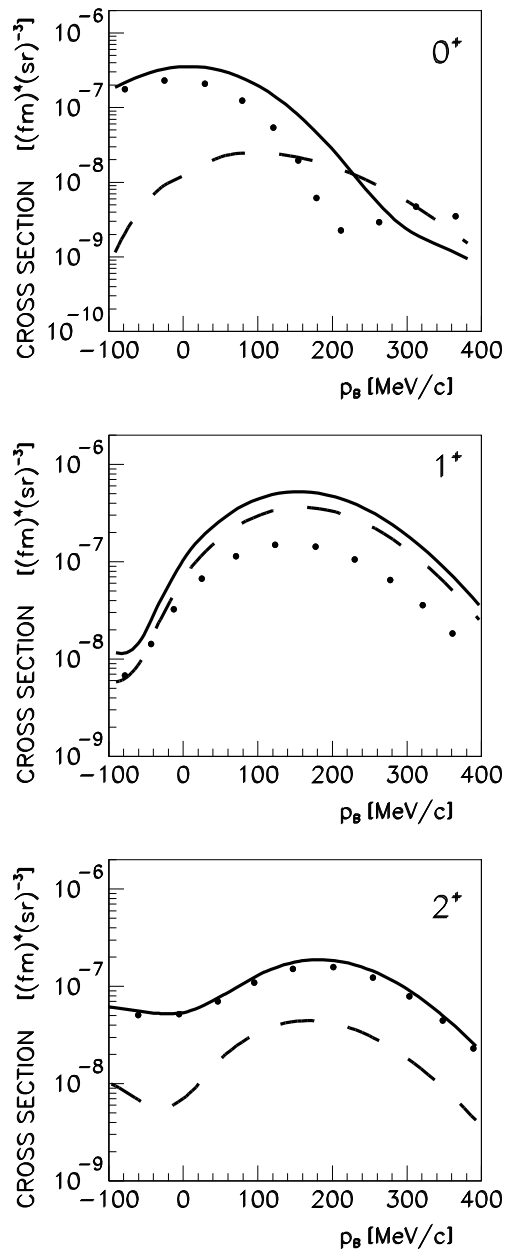


FIG. 1: The differential cross section of the reaction $^{16}\text{O}(e, e'pp)$ to the low-lying states of ^{14}C : the 0^+ ground state, the 1^+ state at 11.31 MeV, and the 2^+ state at 7.67 MeV. A super-parallel kinematics is considered with $E_0 = 855$ MeV, $\omega = 215$ MeV $q = 316$ MeV/c. Different values of the recoil momentum p_B are obtained changing the kinetic energies of the outgoing protons. Positive (negative) values of the recoil momentum refer to situations where \mathbf{p}_B is parallel (anti-parallel) to \mathbf{q} . Separate contributions of the one-body and the two-body Δ current are shown by the dotted and dashed lines, respectively. The solid curves give the final result.

action involving discrete final states which are differently affected by the two reaction processes. The one-body current represents the main contribution for the transitions to the 0^+ and 2^+ states, while the transition to the 1^+ state is dominated by the Δ current. This result is due to the fact that the 0^+ and 2^+ states are reached predominantly by the removal of 1S_0 pairs, whose wave functions are strongly affected by SRC. In contrast, the 1^+ state is reached by the removal of 3P pairs, where SRC only have a minor effect.

The two-nucleon overlap for each transition is characterized by different components of relative and c.m. motion. The relative weights of these components determine the weight of the contributions of the one-body and two-body currents in the cross section and the shape of the recoil-momentum distribution, which is driven by the c.m. orbital angular momentum L of the knocked out pair. This feature is fulfilled in a factorized approach [50], where final-state interaction is neglected and p_B is opposite to the total momentum of the initial nucleon pair, and remains valid when final-state interaction are included [10, 17].

For the transition to the 0^+ state there are the following components of relative motion: 1S_0 , which is combined with a c.m. $L = 0$, 3P_1 , combined with $L = 1$, and 1D_2 , combined with $L = 2$. The contribution from 1D_2 is negligible and the cross section is dominated by the removal of a 1S_0 pair, and thus by SRC, at low values of p_B . The 3P_1 component and thus the Δ current become more important at larger values of the momentum, where the contribution of the c.m. component $L = 0$ is strongly reduced.

The 1^+ state is predominantly obtained from the 3P_0 , 3P_1 , and 3P_2 waves, always combined with a $L = 1$ c.m. wave function. This explains the p -wave shape of the recoil-momentum distribution and the dominant role of the two-body Δ current in the cross section. The components 3P_2 , combined with $L = 3$, and 1D_2 , combined with $L = 2$, are also included in the calculation, but they give a negligible contribution.

For the transition to the 2^+ state there are the following components of relative motion: 1S_0 , which is combined with a c.m. $L = 2$, 3P_1 and 3P_2 , both combined with $L = 1$ and $L = 3$, and 1D_2 , combined with $L = 0$ and $L = 2$. The main contribution is given by the 1S_0 component, which explains the d -wave shape of the momentum distribution and the dominant role of the one-body current in the calculated cross section.

These results do not change the qualitative features of the cross section calculated in Ref. [10]. The quantitative differences are displayed in Fig. 2. These differences are produced by the detailed treatment of LRC in the removal amplitudes and by the new calculation of the defect functions, accounting for SRC, in the present approach. The substantial reduction of the cross section for the 0^+ state at low values of the recoil momentum is produced by the new defect functions, while the increase at higher momenta is the result of the combined

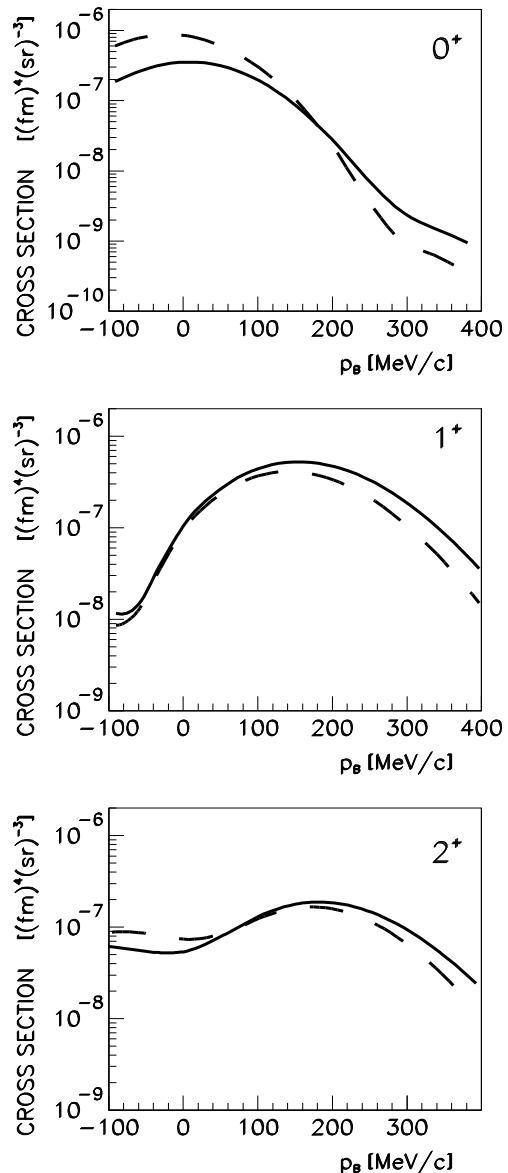


FIG. 2: The differential cross section of the reaction $^{16}\text{O}(e, e'pp)^{14}\text{C}$ for the same transitions and in the same kinematics as in Fig. 1. The solid lines are the results of the present calculation and the dashed lines are the results of Ref. [10].

effect of the new amplitudes and defect functions. Qualitatively similar but smaller effects are found for the 2^+ state. Since the transition to the 1^+ is not very sensitive to SRC, the enhancement of this cross section is predominantly due to the new removal amplitudes. These differ from the ones of Ref. [10] by the contribution from the minor c_{nLSjNL}^i coefficients of Eq. (17).

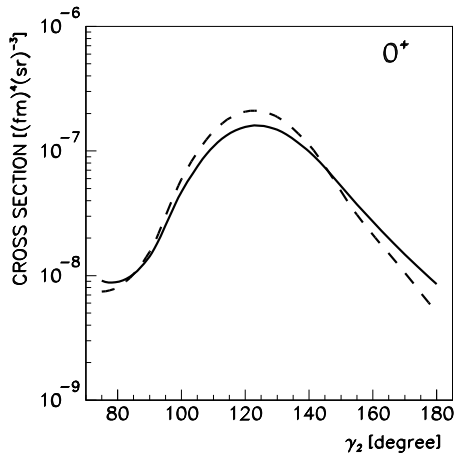


FIG. 3: The differential cross section of the reaction $^{16}\text{O}(e, e'pp)$ to the 0^+ ground state of ^{14}C as a function of the angle γ_2 , between \mathbf{q} and \mathbf{p}'_2 , in a kinematics with $E_0 = 584$ MeV, $\omega = 212$ MeV, $q = 300$ MeV/c, $T'_1 = 137$ MeV and the angle γ_1 , between \mathbf{p}'_1 and \mathbf{q} , $\gamma_1 = -30^\circ$, on the opposite side of the outgoing electron with respect to the momentum transfer. Changing the angle γ_2 , different values of the recoil momentum p_B are explored in the range between -250 and 300 MeV/c, including the zero value at $\gamma_2 \simeq 120^\circ$. Line convention as in Fig. 2.

Another example of the comparison between the results of the present and the previous approach of Ref. [10] is shown in Fig. 3, for the transition to the 0^+ state. Calculations have been performed in a kinematical setting that was included in the experiments carried out at NIKHEF [6, 7]. Also in this kinematics the cross sections are dominated by the removal of a 1S_0 pair, and therefore by the one-body current, at low momenta, whereas the 3P_1 component, and thus the Δ current, becomes important only at larger values of the recoil momentum. The differences between the two results are similar to those found for the same final state in the super-parallel kinematics of Fig. 2: the cross section calculated in the present approach is reduced at low values of p_B , where the cross section in Fig. 3 has the maximum, and it is enhanced at higher values of p_B . Also in this case the reduction is produced by the new defect functions. The effect, however, is smaller than in Fig. 2.

Although the cross sections calculated in the present approach do not change the qualitative features of the results obtained in Ref. [10], the numerical differences confirm that the cross sections are very sensitive to the treatment of correlations in the two-nucleon overlap amplitude. SRC, which are included in the defect functions, predominantly affect the part involving the one-body current. LRC are accounted for in the removal amplitudes of Eq. (17), which determine the weight of the different components of relative and c.m. motion. The shape and size of the cross section as well as the role of the one-body

and two-body currents can thus be affected by both types of correlations. Moreover, it should be noted that a consistent treatment of SRC and LRC, which represents an important merit of the present approach, entails that the two contributions are not independent.

B. The $^{16}\text{O}(e, e'pn)^{14}\text{N}$ reaction

Calculations have been performed for the two lowest-lying discrete states in the residual nucleus ^{14}N , both with positive parity and $T = 0$: the 1_1^+ ground state and the 1_2^+ state at 3.95 MeV.

The differential cross sections of the reaction $^{16}\text{O}(e, e'pn)^{14}\text{N}$ to the two final states in the same super-parallel kinematics already considered in Fig. 1 for the reaction $^{16}\text{O}(e, e'pp)^{14}\text{C}$ are displayed in Fig. 4. Separate contributions of the different terms of the nuclear current are also shown in the figure. For both final states the Δ current gives the most important contribution: it is dominant over the whole momentum distribution shown in the figure for the 1_2^+ state and for recoil-momentum values up to about 100 MeV/c for the ground state. At higher values of p_B the contribution of the one-body current becomes for 1_1^+ comparable and therefore competitive with the one of the Δ current. The contributions of the seagull and pion-in-flight terms are very small and generally much smaller than the one of the one-body current.

The comparison with the corresponding cross sections calculated in the approach of Ref. [15] is shown in Fig. 5. The results of the present approach are always larger than those of Ref. [15]. For the 1_1^+ state the differences are within 20% for recoil-momentum values lower than 100 MeV/c and huge at higher values, where the cross section calculated in the present approach overshoots by an order

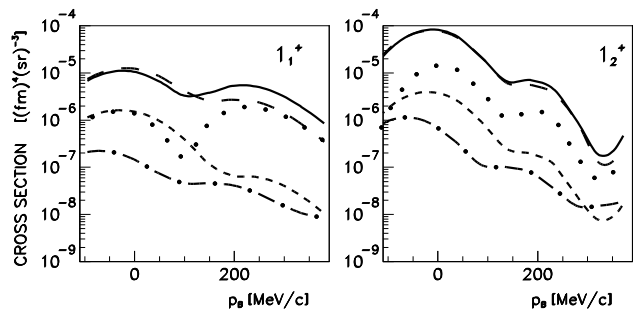


FIG. 4: The differential cross section of the reaction $^{16}\text{O}(e, e'pn)$ to the 1_1^+ ground state and the 1_2^+ state (at 3.95 MeV) of ^{14}N in the same super-parallel kinematics as in Fig. 1. The proton is emitted parallel and the neutron antiparallel to the momentum transfer. Separate contributions of the one-body, seagull, pion-in-flight and Δ current are shown by the dotted, short-dashed, dot-dashed and long-dashed lines, respectively. The solid line gives the total cross section.

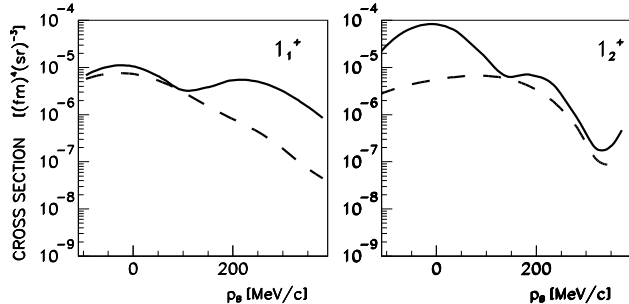


FIG. 5: The differential cross section of the reaction $^{16}\text{O}(e, e'pn)^{14}\text{N}$ for the same transitions and in the same kinematics as in Fig. 4. The solid lines are the results of the present calculation and the dashed lines are the results of Ref. [15].

of magnitude the result of Ref. [15]. A different situation is found in the 1_2^+ state. In this case the present result overshoots by an order of magnitude the cross section of Ref. [15] for values of p_B up to $\simeq 100$ MeV/c, while the differences are strongly reduced at higher momenta.

Therefore, the two models produce cross sections which differ both in size and shape. Also the contributions of the various terms in the nuclear current operator can be different in the two calculations. In both cases the Δ current dominates the reaction to the 1_2^+ state. In contrast, for the 1_1^+ state the main contribution was given in Ref. [15] by the one-body and seagull currents up to $p_B \simeq 100$ MeV/c and by the combined effect of these two terms with the Δ current at higher momenta.

The enhancement of the present cross sections is in part understood by considering the sum of the squared amplitudes in Tab. II, which in Ref. [15] were normalized to the hh-DRPA results for the pp case. The difference in the shape of the cross sections should instead be considered as a result of the different mixing of configurations in the two cases and the fact that the hh-DRPA description considered here allows for pair removal also from particle states. Moreover, the inclusion of fragmentation generates many other coefficients besides those included in Tab. II. We also note that somewhat different models are used to calculate the defect functions in the two calculations, as well as different NN interactions: Bonn-C [40] here and Argonne v_{14} [51] in Ref. [15].

More insight into the cross sections of Fig. 4 and the comparison with the results of Ref. [15] can be obtained from the separate contributions of the partial waves of relative and c.m. motion which are contained in the two-nucleon overlap function. For the transition to the two 1^+ states there are the following relative wave functions: 3S_1 , combined with a c.m. $L = 0$ and $L = 2$, 1P_1 , combined with $L = 1$, 3D_1 , combined with $L = 0$ and $L = 2$, 3D_2 and 3D_3 , both combined with $L = 2$.

The separate contributions of the different partial

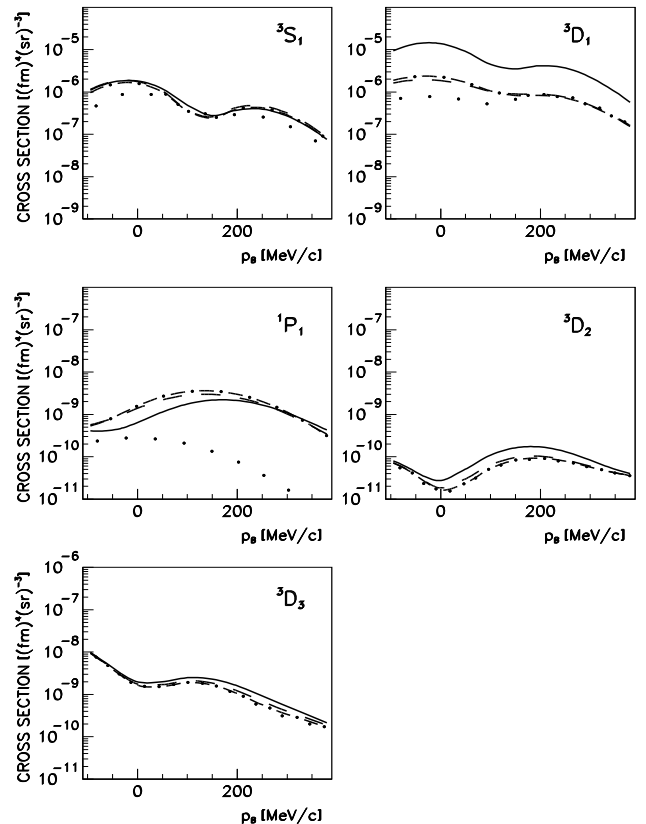


FIG. 6: The differential cross section of the reaction $^{16}\text{O}(e, e'pn)$ to the 1_1^+ ground state of ^{14}N in the same kinematics as in Fig. 4. Separate contributions of different partial waves of relative motion are drawn: 3S_1 , 3D_1 , 1P_1 , 3D_2 , and 3D_3 . The dotted lines give the separate contribution of the one-body current, the dot-dashed lines the sum of the one-body and seagull currents, the dashed lines the sum of the one-body, seagull and pion-in-flight currents and the solid lines the total result, where also the contribution of the Δ current is added.

waves of relative motion for the transition to the ground state of ^{14}N are displayed in Fig. 6. These results can be compared with those shown in Fig. 4 of Ref. [15]. Only a very small contribution is obtained from the 1P_1 , 3D_2 , and 3D_3 waves. The 1P_1 contribution was practically negligible also in the approach of Ref. [15], where the 3D_2 and 3D_3 waves were not included in the calculation. The most important contribution is given in Fig. 6 by the 3D_1 component. This partial wave is dominated by the Δ current, which enhances the cross section by about an order of magnitude at low recoil-momentum values. The one-body, and also the seagull current, play the main role in 3S_1 , but the contribution of this partial wave is significant only at large values of the recoil momentum. This explains the result in Fig. 5, where the Δ current is dominant at low momenta and the one-body

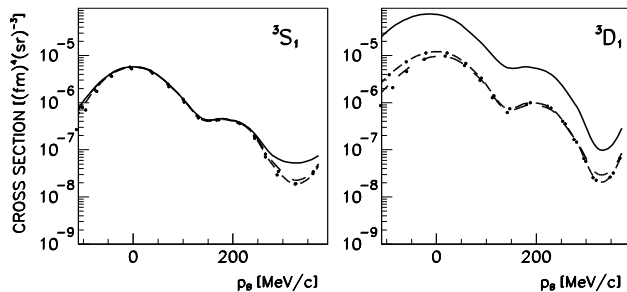


FIG. 7: The differential cross section of the reaction $^{16}\text{O}(e, e'pn)$ to the 1_2^+ state of ^{14}N in the same kinematics as in Fig. 4. Separate contributions of the 3S_1 and 3D_1 partial waves of relative motion are displayed. Line convention as in Fig. 6.

current is important only above 100 MeV/c. In contrast, in Ref. [15] the one-body and the seagull current were the main terms at low momenta, where the contribution of 3S_1 was larger than the one of 3D_1 . The shape of the final cross section in Fig. 5 is obtained from the combination of the c.m. wave functions with $L = 0$ and $L = 2$. In the present calculation the $L = 2$ components turn out to be more relevant than in Ref. [15].

For the 1_2^+ state only the contributions of the most important partial waves, 3S_1 and 3D_1 , are drawn in Fig. 7. The one-body current is dominant in 3S_1 and the Δ current in 3D_1 , where it enhances the cross section by about an order of magnitude. Therefore, the final cross section is dominated by the Δ current in the 3D_1 component. As regards the shape, the contribution of the $L = 0$ wave functions of the c.m. motion is larger than in Ref. [15].

A crucial contribution to proton-neutron emission is given by tensor correlations. These correlations, which are mainly due to the strong tensor components of the pion-exchange contribution to the NN interaction, are very important in the wave function of a proton-neutron pair, while they are much less important for a proton-proton pair. Tensor correlations are accounted for in the defect functions and produce correlated wave functions also for channels for which the uncorrelated wave function vanishes. In Ref. [15] the effects of tensor correlations were investigated comparing, for the 3D_1 relative wave function, the contribution of the components already present in the uncorrelated wave function with the one of the components due to the coupling induced by tensor correlations and which are not present in the uncorrelated wave function. Even if tensor correlations are present in all the components, this was a simple way to give an idea of the relevance of their contribution.

Likewise here we have performed a calculation of the cross sections neglecting the defect functions produced by tensor correlations in those channels for which the uncorrelated wave function vanishes. The results for the 1_1^+

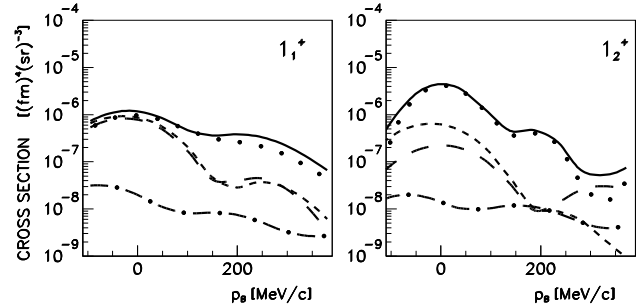


FIG. 8: The differential cross section of the reaction $^{16}\text{O}(e, e'pn)^{14}\text{N}$ for the same transitions, in the same kinematics and with the same line convention as in Fig. 4. The defect functions produced by tensor correlations in those channels for which the uncorrelated wave function vanishes have been switched off in the calculations.

and 1_2^+ states are displayed in Fig. 8. A dramatic reduction of the cross section by about one order of magnitude is obtained, for both transitions, in comparison with the complete calculations of Fig. 4. This result clearly indicates the dominant role of tensor correlations in $(e, e'pn)$. The reduction is large for all the terms of the nuclear current, but it is huge for the Δ current, whose contribution is reduced by about one order of magnitude in 1_1^+ and up to about two orders of magnitude in 1_2^+ . Therefore, the Δ current, which dominates the complete result of Fig. 4, gives in Fig. 8 a contribution comparable to the one of the seagull current and the one-body current becomes for both states the most important term in the cross section. This result can be seen in more detail in Fig. 9, where the separate contributions of the most important partial waves, 3S_1 and 3D_1 , are displayed in the calculation where the defect functions produced by tensor correlations are neglected. The contribution of 3S_1 is practically the same as in Figs. 6 and 7, while the contribution of 3D_1 , is dramatically reduced. The reduction is particularly strong, of about two orders of magnitude, for the 1_2^+ state. Therefore, in the calculations of Figs. 8 and 9 the most important contribution is given by 3S_1 and by the one-body current.

These results indicate that tensor correlations dominate the $(e, e'pn)$ cross section. They affect all the terms of the nuclear current, but produce a particularly strong enhancement of the Δ -current contribution. This means that also a situation where the cross section is dominated by the Δ current might provide an interesting and useful tool to investigate tensor correlations. Such a situation can be realized in the $(e, e'pn)$ reaction considered here and can be also expected in the (γ, pn) reaction, which therefore deserves further investigation in the future. Naturally, the ultimate arbitration of these conjectures must be given by the experimental data.

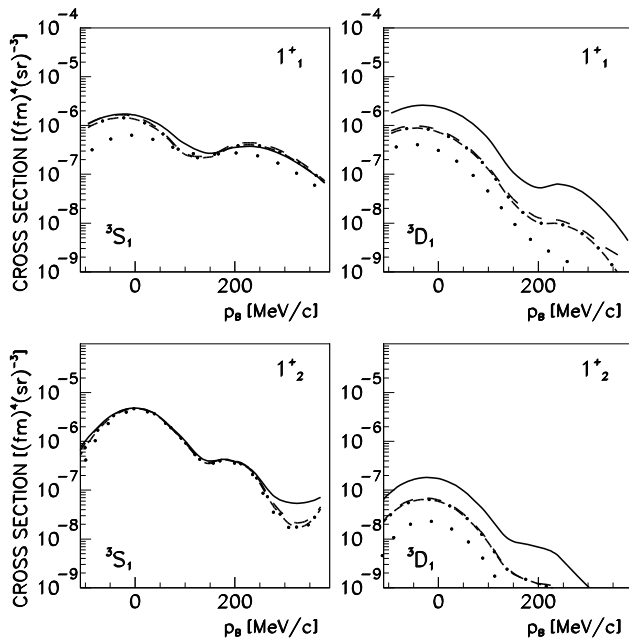


FIG. 9: The differential cross section of the reaction $^{16}\text{O}(e, e'pn)$ for the same transitions and in the same kinematics as in Fig. 4. The defect functions produced by tensor correlations in those channels for which the uncorrelated wave function vanishes have been switched off in the calculations. Separate contributions of the 3S_1 and 3D_1 partial waves of relative motion are displayed. Line convention as in Fig. 6.

V. CONCLUSIONS

The $^{16}\text{O}(e, e'pN)$ cross sections have been computed for the transitions to the ground state, 1^+ and 2^+ levels of ^{14}C and to the lowest two isoscalar 1^+ states of ^{14}N . Both the emissions of a pp or a pn pair have been computed by employing the same model for the nuclear structure and the reaction mechanism.

The overlap functions have been computed by partitioning the Hilbert space, in order to determine the contribution of LRC and SRC separately. The LRC, describing the collective motion at low energy, are computed within a model space by solving the hh-DRPA equations and the effects of fragmentation of the sp strength are taken into account (self-consistently). The inclusion of SRC is accomplished by determining appropriate defect functions. The present work, improves the treatment of the defect functions employed in the $(e, e'pp)$ calculations of Refs. [10, 25] and applies the same many-body approach to the pn emission.

The $^{16}\text{O}(e, e'pp)$ cross sections are found to be similar to the results of Ref. [10]. The transitions to the 0^+ g.s. and the 2^+ state of ^{14}C are shown to be sensitive to the one-body currents and, therefore, to the effects of SRC. This is in accordance with previous works. At small recoil

momentum, the reaction rate is found to be lower than the one of Ref. [10]. This is due to the different treatment of the defect functions employed in this work. At high recoil momentum, instead, all the computed $^{16}\text{O}(e, e'pp)$ cross sections show a slight enhancement due to the interference between the LRC amplitudes and the new defect functions. However, the main conclusions of previous studies of this reaction are not changed, including the sensitivity of the effects of correlations on the choice of the final state.

In contrast, the results for the $^{16}\text{O}(e, e'pn)$ reaction are found to deviate from previous calculations [15]. This is principally due the different many-body approach employed in this work, which accounts for the possibility of extracting two nucleons from orbitals above the Fermi energy (which are partially occupied in the correlated g.s.). This results in a drastic change of the shape of the cross section. Moreover, the normalization of the two-hole overlap amplitude is higher in the hh-DRPA approach for the emission of a pn pair than for a pp pair. The present calculations suggest that both the transitions to the 1^+_1 and 1^+_2 states of ^{14}N are dominated by the contribution from the Δ current, except for the 1^+_1 at high recoil momentum where the one-body current is also important. This situation is different from the results of Ref. [15] showing that the reaction rate depends sensitively on the details of the LRC as well. The present calculation of LRC effects appears to be the most complete one performed for this specific transition. However, more work on nuclear structure may be required to check the accuracy of the results obtained. Both the results of this work and of Ref. [15], suggest that the effect of tensor correlations are important for the pn emission (even dominant in this case) and that they influence the cross section principally through the Δ current. The higher cross section obtained here is a consequence of the interplay between the details of LRC and the tensor correlations included in the defect functions. This feature could be used to investigate the effects of tensor correlations by means of $(e, e'pn)$ and (γ, pn) measurements.

In general, all the transitions studied show a strong sensitivity to the details of nuclear structure and confirm that the importance of different types of correlations and reaction mechanisms is particular to the chosen final state. While more work can be done on the theoretical side to improve the calculation of these cross sections [22, 23, 35], it appears clear that two-nucleon emission experiments should be considered as a very powerful tool to probe various aspects of nuclear correlations, even beyond the SRC.

Acknowledgments

This work was supported in part by the U.S. National Science Foundation under Grant No. PHY-0140316 and in part by the Natural Sciences and Engineering Research Council of Canada (NSERC).

-
- [1] S. C. Pieper and R. B. Wiringa, *Ann. Rev. Nucl. Part. Sci.* **51**, 53 (2001)
- [2] J. Morales, V. R. Pandharipande, and D. G. Ravenhall, *Phys. Rev. C* **66**, 054308 (2002).
- [3] Y. Dewulf, W. H. Dickhoff, D. Van Neck, E. R. Stoddard, and M. Waroquier *Phys. Rev. Lett.* **90**, 152501 (2003).
- [4] W. H. Dickhoff and C. Barbieri *Prog. Part. Nucl. Phys.* (2004), in press [nucl-th/0402034].
- [5] C. J. G. Onderwater et al., *Phys. Rev. Lett.* **78** 4893 (1997).
- [6] C. J. G. Onderwater *et al.*, *Phys. Rev. Lett.* **81**, 2213 (1998).
- [7] R. Starink *et al.*, *Phys. Lett. B* **474**, 33 (2000).
- [8] G. Rosner, *Prog. Part. Nucl. Phys.* **44**, 99 (2000).
- [9] J. Ryckebusch, V. Van der Sluys, K. Heyde, H. Holvoet, W. Van Nespen, and M. Waroquier, *Nucl. Phys.* **A624**, 581 (1997).
- [10] C. Giusti, F. D. Pacati, K. Allaart, W. J. W. Geurts, W. H. Dickhoff, and H. Mütter, *Phys. Rev. C* **57**, 1691 (1998).
- [11] J. R. M. Annand, *et al.*, MAMI proposal Nr: A1/5-98.
- [12] I. Sick, *et al.*, Jlab-Proposal E97-006, (1997).
- [13] D. Rohe, *Eur. Phys. J.* **A17**, 439 (2003), (*Conference proceeding on Electron-Nucleus Scattering VII in Elba 2002*); in *Proceedings of the 6th Workshop on “e-m Induced Two-Hadron Emission”*, eds. A. Braghieri, C. Giusti, and P. Grabmayr (University of Pavia, Italy 2004), p. 58.
- [14] C. Barbieri and L. Lapikás, in *Proceedings of the 6th Workshop on “e-m Induced Two-Hadron Emission”*, eds. A. Braghieri, C. Giusti, and P. Grabmayr (University of Pavia, Italy 2004), p. 68, and [nucl-th/0401010].
- [15] C. Giusti, H. Mütter, F. D. Pacati, and M. Stauf, *Phys. Rev. C* **60**, 054608 (1999).
- [16] J. Ryckebusch and W. Van Nespen, [nucl-th/0312056].
- [17] C. Giusti and F. D. Pacati, *Nucl. Phys.* **A615**, 373 (1997).
- [18] P. Wilhelm, H. Arenhövel, C. Giusti, and F. D. Pacati, *Z. Phys. A* **359**, 467 (1997).
- [19] C. Giusti and F. D. Pacati, *Nucl. Phys.* **A641**, 297 (1998).
- [20] C. Giusti and F. D. Pacati, *Phys. Rev. C* **67**, 044601 (2003).
- [21] D. Knödler, H. Mütter, and P. Czerski, *Phys. Rev. C* **61**, 064603 (2000).
- [22] M. Schwamb, S. Boffi, C. Giusti, and F. D. Pacati, *Eur. Phys. J.* **A 17**, 7 (2003).
- [23] M. Schwamb, S. Boffi, C. Giusti, and F. D. Pacati, *Eur. Phys. J.* (2004), in press [nucl-th/0307003].
- [24] M. Schwamb, *et al.* in preparation.
- [25] W. J. W. Geurts, K. Allaart, W. H. Dickhoff, and H. Mütter, *Phys. Rev. C* **53**, 2207 (1996).
- [26] C. Barbieri and W. H. Dickhoff, *Phys. Rev. C* **63**, 034313 (2001).
- [27] C. Barbieri and W. H. Dickhoff, *Phys. Rev. C* **65**, 064313 (2002).
- [28] W. J. W. Geurts, K. Allaart, W. H. Dickhoff, and H. Mütter, *Phys. Rev. C* **54**, 1144 (1996).
- [29] S. Boffi, C. Giusti, F. D. Pacati, and M. Radici, *Electromagnetic Response of Atomic Nuclei*, Oxford Studies in Nuclear Physics (Clarendon Press, Oxford, 1996); S. Boffi, C. Giusti, and F. D. Pacati, *Phys. Rep.* **226**, 1 (1993).
- [30] C. Giusti and F. D. Pacati, *Nucl. Phys.* **A535**, 573 (1991).
- [31] R. D. Peccei, *Phys. Rev.* **176**, 1812 (1968); **181**, 1902 (1969).
- [32] A. Nadasen *et al.*, *Phys. Rev. Phys. Rev. C* **23**, 1023 (1981).
- [33] H. Mütter and P. U. Sauer, in *Computational Nuclear Physics*, K.-H. Langanke, J. A. Maruhn and S. E. Koonin, eds. (Springer, New York, 1993).
- [34] M. Hjorth-Jensen, T. T. S. Kuo and E. Osnes, *Phys. Rep.* **261**, 125 (1995).
- [35] C. Barbieri and W. H. Dickhoff, *Phys. Rev. C* **68**, 014311 (2003).
- [36] M. G. E. Brand, K. Allaart, and W. H. Dickhoff, *Phys. Lett.* **B214**, 483 (1988).
- [37] M. G. E. Brand, K. Allaart, and W. H. Dickhoff, *Nucl. Phys.* **A509**, 1 (1990).
- [38] M. G. E. Brand, G. A. Rijsdijk, F. A. Muller, K. Allaart, and W. H. Dickhoff, *Nucl. Phys.* **A531**, 253 (1991).
- [39] G. A. Rijsdijk, K. Allaart, and W. H. Dickhoff, *Nucl. Phys.* **A550**, 159 (1992).
- [40] R. Machleidt, *Adv. Nucl. Phys.* **19**, 191 (1989).
- [41] A. L. Fetter and J. D. Walecka, *Quantum Theory of Many-Particle Physics* (McGraw-Hill, New York, 1971).
- [42] A. A. Abrikosov, L. P. Gorkov and I. E. Dzyaloshinski, *Methods of Quantum Field Theory in Statistical Physics* (Dover, New York, 1975).
- [43] A. R. Edmonds, *Angular Momentum in Quantum Mechanics* (Princeton University Press, 1957).
- [44] P. J. Brussaard and P. W. M. Glaudemans, *Shell-Model Applications in Nuclear Spectroscopy* (North-Holland, Amsterdam, 1977).
- [45] T. A. Brody and M. Moshinsky *Tables of Transformation Bracket for Nuclear Shell-Model Calculations* (Universidad Autonoma de Mexico, 1960).
- [46] M. Leuschner *et al.*, *Phys. Rev. C* **49**, 955 (1994).
- [47] M. Radici, W. H. Dickhoff, and E. R. Stoddard, *Phys. Rev. C* **66**, 014613 (2002).
- [48] M. K. Gaidarov, *et al.*, *Phys. Rev. C* **61**, 014306 (2000).
- [49] F. Ajzenberg-Selove, *Nucl. Phys. A* **523**, 1 (1991).
- [50] K. Gottfried, *Nucl. Phys.* **5**, 557 (1958).
- [51] R. B. Wiringa, R. A. Smith, and T. L. Ainsworth, *Phys. Rev. C* **29**, 1207 (1984).